Observation of longitudinal optical–transverse optical splitting for E-symmetry phonons in Te by coherent phonon spectroscopy

2005 J. Phys.: Condens. Matter 17 3015

(http://iopscience.iop.org/0953-8984/17/19/015)

INSTITUTE OF PHYSICS PUBLISHING JOURNAL OF PHYSICS: CONDENSED MATTER

J. Phys.: Condens. Matter **17** (2005) 3015–3023 doi:10.1088/0953-8984/17/19/015

Observation of longitudinal optical–transverse optical splitting for E-symmetry phonons in Te by coherent phonon spectroscopy

O V Misochko[1], M V Lebedev[1] and T Dekorsy[2]

[1] Institute of Solid State Physics, Russian Academy of Sciences, 142432 Chernogolovka, Moscow region, Russia
[2] Institute for Ion Beam Physics and Materials Research, Forschungszentrum Rossendorf, PO Box 510119, D-01314 Dresden, Germany

Received 22 December 2004
Published 29 April 2005
Online at stacks.iop.org/JPhysCM/17/3015

Abstract

We report on the femtosecond time-resolved detection of coherent phonons in single-crystal tellurium. For different crystallographic faces a detection scheme is employed which is sensitive to the anisotropic part of the Raman tensor. In this scheme we observe all three Raman allowed phonons, i.e. one of A_1 and two of E symmetry. Furthermore, for both doubly degenerate E-symmetry modes obtained from different crystallographic faces, longitudinal optical–transverse optical splitting is observed. In addition, we show that even in the low fluence regime the frequency of the fully symmetric phonon in Te is chirped and that it demonstrates an anomalous dependence on the pump fluence.

Time-resolved spectroscopy offers in many cases a new twist to phenomena observed by conventional, non-time-resolved spectroscopic techniques. Although the technique is not new, the development of ultrafast lasers has opened up a wide range of research, including testing and measurement of laser-induced phase transitions [1], the generation of non-classical lattice states [2], and the quantum condensation of quasiparticles [3]. Ultrashort optical pulses of sub-picosecond duration enable studies of a great variety of ultrafast phenomena, among which are the generation and time-resolved detection of coherent phonons. Many experiments have been carried out and theories have been developed to explain the physics behind coherent lattice dynamics [2, 4, 5]. It has been firmly established that Raman-active phonons of full and lower symmetry are generated following ultrafast photoexcitation of a variety of solids. However, no time-resolved experimental study to date has monitored spectral features which are, for some reasons, absent in spontaneous Raman scattering spectra. Such a study may contribute to a better understanding of coherent phonons and the mechanisms relevant for their generation. Therefore, we performed a detailed analysis of coherent phonons excited in single-crystal tellurium under different scattering configurations. Measuring transient reflectivity values from different crystallographic faces allows the detection of phonons of different symmetry by

utilizing various detection schemes. From *anisotropic* transient reflectivity data of tellurium we can directly observe the LO–TO splitting in the time domain for low symmetry phonons, excited from different crystallographic faces.

Different crystallographic faces of a Czochralski-grown single crystal of Te are excited with 830 nm pulses from a Ti:sapphire system delivering 65 fs pulses at a repetition rate of 80 MHz. We use nearly collinear pump and probe pulses which are focused to a 100 μm spot on the chosen crystal surface. We acquire reflectivity transients using a fast-scan technique, where the time delay is achieved via a retro-reflector mounted on a shaker oscillating at approximately 40 Hz. This technique gives sensitivity to relative reflectivity changes $\Delta R/R$ better than 10^{-6}. The *isotropic* and *anisotropic* transient reflectivities of Te are measured under ambient conditions. The term *isotropic* refers to a non-polarization analysed detection of transient reflectivity changes, whereas the term *anisotropic* refers to a polarization analysis of the reflected probe beam. The latter detection is often referred to as reflective electro-optic sampling of coherent phonons, since it monitors polarization changes perpendicular to the surface via the linear electro-optic or Pockels effect [5]. To access the anisotropic reflectivity change, after reflecting from the sample, the probe beam is analysed into polarization components parallel and perpendicular to that of the pump, $\Delta R_{\parallel}$ and $\Delta R_{\perp}$, and detected with two photodiodes. The photocurrents of the two diodes are subtracted, and their amplified difference $\Delta R(t) = \Delta R_{\perp}(t) - \Delta R_{\parallel}(t)$ is recorded as a function of the pump–probe delay. In the conventional sampling no polarization analysis is performed; therefore $\Delta R(t) = R(t) - R(T \prec 0)$. Further details of the experimental technique can be found elsewhere [2, 5].

Tellurium crystallizes with three atoms per unit cell. It is characterized by infinite helical chains, with three atoms per turn, oriented parallel to the c axis. Group theory analysis for Te predicts four zone centre optical phonons of which three are Raman active. These are two doubly degenerate E′ and E″ modes and one non-degenerate A_1 mode. The A_1 phonon, which corresponds to the symmetric intrachain dilation and compression normal to the chain axis, involves bond-length and bond-angle distortions. This fully symmetric phonon preserves the crystal symmetry and is only Raman active. The E phonons correspond to axial helix compression and asymmetric (normal to the helix axis) dilation. These are also intrachain phonons that, however, lower the crystal symmetry, and are both Raman and infrared active. All these phonons (A_1 and E symmetry) have been detected and studied in the frequency domain [6, 7] as well as in the time domain [8–12]. The Raman tensors arising from the deformation potential electron–phonon interaction for D_3 symmetry are

$$\mathrm{A}_1 = \begin{pmatrix} a & & \\ & a & \\ & & b \end{pmatrix}, \qquad \mathrm{E}(x) = \begin{pmatrix} c & & \\ & -c & d \\ & d & \end{pmatrix}, \qquad \text{and}$$
$$\mathrm{E}(y) = \begin{pmatrix} & -c & -d \\ -c & & \\ -d & & \end{pmatrix} \tag{1}$$

where x, y, and z are the binary, bisectrix, and trigonal axes, respectively. If an electric field is associated with an ion displacement (as is the case for the E phonons), the tensors must be modified because of the electro-optic effect[3]. The associated effective charge can be, in principle, measured by means of spontaneous Raman scattering through a splitting of the E doublets into phonons of longitudinal and transverse polarization. This is possible since the

[3] Raman scattering occurs by means of two basic mechanisms: the displacement mechanism, a modulation of the optical polarizability by the atomic displacements (quite often called the deformation potential mechanism) and the field mechanism, a modulation of the polarizability by the macroscopic longitudinal electric field (quite often called the electro-optic mechanism).

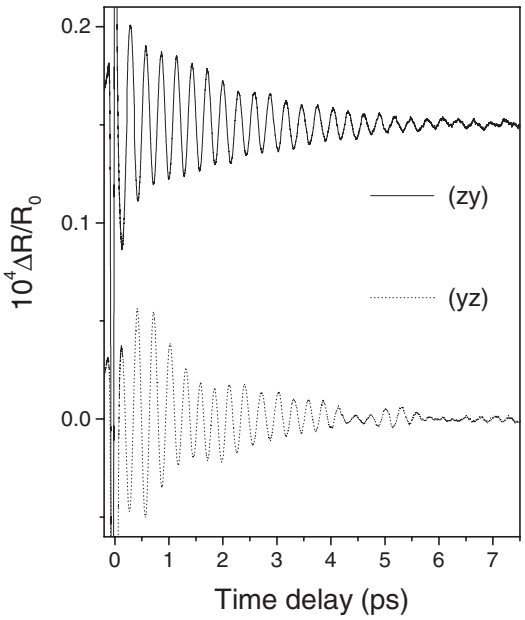

Figure 1. Transient differential reflectivity versus time delay obtained with the anisotropic detection scheme for two different polarizations of the pump beam within the *bc* face. Upper trace: pump polarization parallel to the trigonal axis, probe polarization parallel to the bisectrix axis. Bottom trace: pump parallel to the bisectrix axis, probe parallel to the trigonal axis. The pump fluence is 5.4 mJ cm^{-2}.

phonons with a wavevector of the order of the inverse penetration depth can be probed in a Raman process. Nevertheless, accurate Raman studies [6, 7] failed to directly detect splitting at room temperature for both the E″ mode with small effective charge and for the E′ mode with a large effective charge; therefore the splitting was deduced from either the comparison with IR data [6], or the LO frequencies derived on the basis of the analysis of the extraordinary phonons (mixed $A_2 + E$ modes) [7]. In both Raman works the lack of LO phonons at room temperature was explained by the cancellation (destructive interference) due to the different signs in the deformation potential and electro-optic contribution to the Raman tensor [6, 7]. However, at $T = 90$ K the tiny splitting of 0.018 THz (=0.6 cm^{-1}) was observed for the E″ mode from the comparison of unpolarized and polarized spectra taken from the *y* face.

In figure 1 two (of the total four) time-resolved measurements of the anisotropic reflectivity of the *bc* face are presented. The mono-exponential decaying electronic background has been subtracted, thus revealing just the coherent phonon-induced signal. We find that only in the case where the pump is polarized along the trigonal axis does the time-resolved signal reveal a regular oscillation which implies that a single phonon frequency is generated. For three other cases, quite pronounced beats are observed. The Fourier transform, which is a measure of the frequency and amplitude of the coherent phonon oscillations, shows that for these geometries four or even five different phonons are coherently excited. Thus, the multiple structures observed for certain experimental geometries are the manifestation of a modified screening induced by photoexcited carriers. Figures 2 and 3 depict the Fourier transforms of all four time-resolved traces taken in various geometries. The A_1 mode appears in all of these configurations, and for the case $e_{\text{pump}} \parallel z$ (e—unit vector of the electric field) it is the only mode in the spectrum. For the case $e_{\text{pump}} \parallel y$ taken from the same *bc* plane, one can see

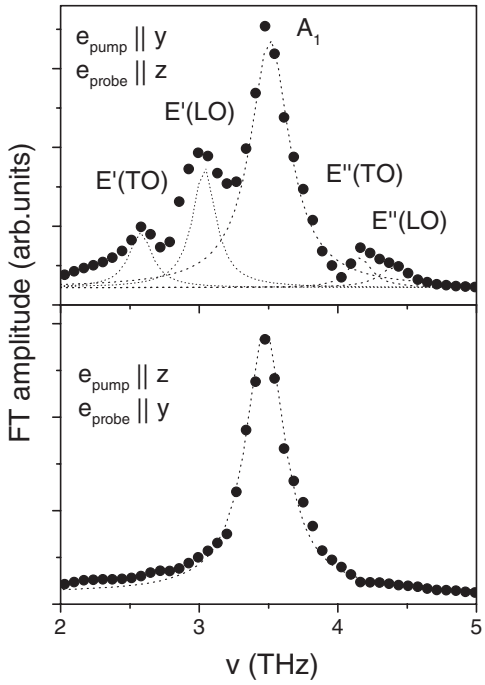

Figure 2. Fourier transformed spectra for the oscillating parts of transient reflectivity obtained from the *bc* face with the pump fluence of 6.0 mJ cm^{-2}. The dotted lines are Lorentzian fits to each oscillation (the fitting parameters are summarized in table 1).

additionally four modes of which two can be ascribed to LO phonons. The amplitude of the LO mode of E′ symmetry is larger than that of the TO counterpart, whereas for E″ symmetry the situation is reversed. By comparing our data to those of [9], where only E′ phonons were detected, we can ascribe the differences to either distinct resonance conditions (1.6 versus 2 eV photon energy), or to an angular dependence (the polarization of the pump was not controlled relative to the crystal axis in [9]). In the spectra obtained from the basal face, the E″ modes are very broad and spectrally unresolved (even though the line shape is indicative of a larger amplitude for TO modes). As to the modes of E′ symmetry, we detect that the LO amplitude is larger (as compared to the TO amplitude) when the pump polarization is along the bisectrix axis and smaller when the polarization is along binary axis; see figure 3. The fitting parameters for all phonons observed from the basal plane are summarized in table 1. Somewhat lower frequencies for all modes except the E″ (LO) phonon (as compared to the frequency domain data) are caused by the fact that the 'instantaneous frequency' of a phonon drifts in time for pump–probe experiments [3, 10]. It should be mentioned that no LO phonons were observed from the basal plane in [9]. We tentatively explain this fact by a lower fluence used in [9], since for the low fluence excitation in our case the contribution for longitudinal modes was suppressed and the spectra were identical to those observed from the basal plane in [9].

The explanation of the results obtained is straightforward: as follows from Raman selection rules, orienting the pump polarization along the trigonal axis restricts the generation to the fully symmetric phonon only, whereas the situations where the pump polarization coincides with the binary or bisectrix axis allow the excitation of both non-degenerate and degenerate modes owing to their nonzero diagonal matrix elements. This explains the different numbers of modes detected for the different scattering configurations. The appearance of LO modes

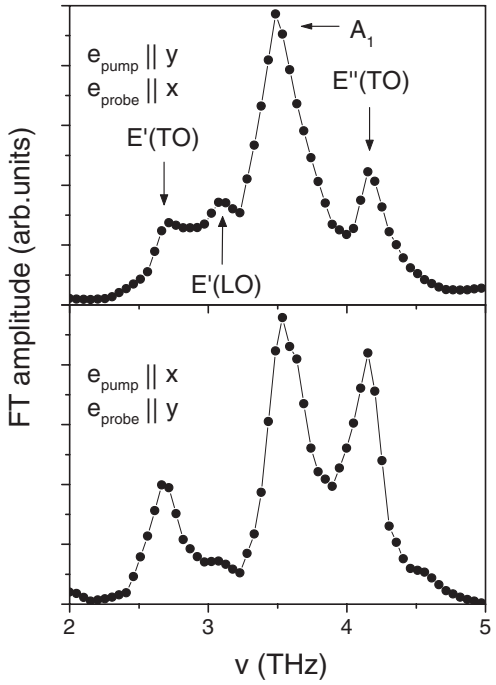

Figure 3. Fourier transformed spectra for the oscillating parts of transient reflectivity obtained from the basal *ab* face with the pump fluence of 6.0 mJ cm^{-2}.

Table 1. Phonon frequencies and linewidths obtained from the *bc* face of Te. The frequencies obtained in the Raman and IR experiments at room temperature (see [18]) are shown in square brackets.

	E′ (TO)	E′ (LO)	A_1	E″ (TO)	E″ (LO)
ν (THz)	2.58 [2.76]	3.04 [3.09]	3.51 [3.61]	4.17 [4.21]	4.31 [4.26]
$\Delta\nu$ (THz)	0.19	0.21	0.34	0.2	0.25

in the spectra is most likely due to their coupled character arising from the hybridization with optically excited plasmons. Such a hybridization is absent in spontaneous Raman scattering and it appears only in the time domain since, assuming strictly linear absorption, the highest pump fluence ($\approx$0.7 mJ cm^{-2}) corresponds to a maximum excited carrier density at the surface of 5.7×10^{20} cm^{-3}, i.e. about 0.35% of the valence electrons in Te being excited. In other words, the electron plasma, generated by an intense pump pulse, modifies the ratio between the deformation potential and electro-optical contributions, thus preventing their destructive interference. Such a conclusion is supported by the fact that the LO phonon is absent at the lowest fluence excitation, where the photogenerated carrier density is low. We also note that the main contribution for the LO phonon comes from relatively short delay times. For long delay times, as evidenced by a Fourier transform in a smaller time window, the contribution of the LO phonon is negligible even for the relatively high fluence excitation. A possible reason for the non-observation of the LO mode for long delay is that, if the LO mode excitation is weak in the absence of a plasma, this is also the case for the detection. From this argument, the LO phonon mode could be not detected by the weak probe pulse for long delay times just due to plasma relaxation.

Since TO and LO phonons are observed simultaneously, from their amplitude ratio the Faust–Henry coefficient C can be estimated [13]:

$$\frac{d_{\mathrm{LO}}}{d_{\mathrm{TO}}} = \left(1 - \frac{\omega_{\mathrm{LO}}^2 - \omega_{\mathrm{TO}}^2}{C\omega_{\mathrm{TO}}^2}\right), \tag{2}$$

ω_{LO} and ω_{TO} being the phonon frequencies, d_{LO} and d_{TO} the corresponding components of the Raman scattering tensor. As follows from equation (2), Raman efficiency for LO phonon scattering is enhanced ($C < 0$) or reduced ($C > 0$) with respect to that for the TO phonon depending on the sign and magnitude of the Faust–Henry coefficient C. As follows from [13] the Faust–Henry coefficient is given by

$$C = \frac{e^*\hat{\varepsilon}_L(\partial\chi/\partial u)\hat{\varepsilon}_S}{\mu\omega_{\mathrm{TO}}^2\hat{\varepsilon}_L(\partial\chi/\partial E)\hat{\varepsilon}_S} \tag{3}$$

where e^* is the dynamical charge, μ is the reduced mass, $\partial\chi/\partial u$ is the deformation potential, $\partial\chi/\partial E$ is the electro-optical coefficient, $\hat{\varepsilon}_L$ and $\hat{\varepsilon}_S$ are the unit polarization vectors for the incoming and outgoing photons. Since according to equation (3) C is a measure of the ratio of the 'mechanical' strength of bonds (the deformation potential) to the electric (Fröhlich) one in the electron–phonon interaction [13], it is seen that photoinduced carriers generated by the intense pump pulse result in the redistribution of these contributions.

The large TO–LO splitting (0.4 THz or 13 cm^{-1}) of the E′ phonon corresponds to a larger effective charge of $2.2e$ as compared to that of the E″ phonon with a TO–LO splitting of 0.15 THz (5 cm^{-1}) and an effective charge of $0.32e$ [14]. In fact, a very broad structure is observed in the expected frequency range of the E″ (LO) mode. While the appearance of the A_1 mode is natural for the bc crystal plane, the peak at the fully symmetric phonon frequency in the Fourier transformed signals obtained from the basal plane comes as a surprise. Indeed, for this geometry the symmetry considerations predict no fully symmetric signal due to the equality of xx and yy matrix elements of the Raman tensor. The reason for the appearance of the A_1 mode may be a slight misorientation of the basal plane or strain in the soft tellurium crystals. In the former case, the A_1 mode may appear due to different magnitudes of the zz and xx (yy) matrix elements, while in the latter case, the strain leads to different magnitudes of the xx and yy matrix elements, making the bisectrix and binary directions non-equivalent. Further experimental work is needed to make a final decision on the matter.

Early experimental work on Te demonstrated a softening of the A_1 mode for high excited carrier densities [10]. Motivated by this finding, Tangney and Fahy performed *ab initio* calculations that revealed a linearly decreasing dependence of the A_1 phonon frequency on the excited carrier density, in agreement with experiments [15]. The calculations also indicated that intense photoexcitation of tellurium drives the lattice toward a band-crossing transition, which has been successfully observed quite recently [12]. Since the order parameter for this transition is the A_1 mode, which behaves anomalously as the transition is approached, such a behaviour deserves further study. In order to further explore the role of the A_1 mode we measured the pump dependence of the coherent phonons in a low fluence regime using the isotropic detection scheme. A summary of the pump dependence is presented in figure 4. Surprisingly, many of the features, which are thought to be intrinsic only to the high fluence regime [10], are already present at low fluence. Among them are the dependence of the frequency and the dephasing rate on the pump fluence and a frequency chirp. A linear regression fit through the peak frequency data shows that even for the low fluence experiments the A_1 phonon frequency softens with increasing excitation fluences at a rate of -0.065 THz mJ^{-1} cm^2, in agreement with previous high fluence measurements [10]. The A_1 mode softening with higher fluence is indicative of intrachain bond weakening under photoexcitation while interchain interactions

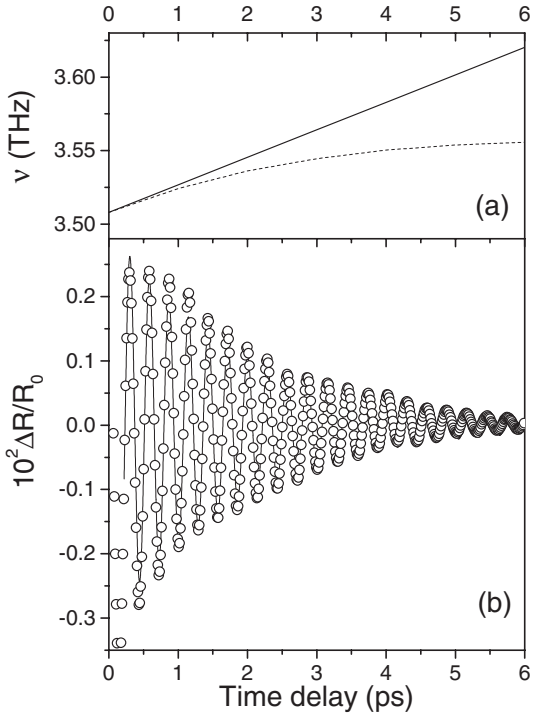

Figure 4. (a) Instantaneous frequency of the A_1 oscillation (b) obtained from the *bc* face versus time delay. In the upper panel (a) the solid line corresponds to the frequency obtained with a linear non-decaying chirp, whereas the dotted line was obtained with a decaying chirp. In the bottom panel open symbols are the experimental points (every tenth point is shown), while the solid line is a fit including the non-decaying chirp.

become stronger thereby reducing the overall crystal anisotropy. It is well known [16] that the frequency of this mode decreases significantly under hydrostatic compression. Making a comparison to high pressure experiments that reported a decrease of the ratio of interchain–intrachain bond lengths, we conclude that photoexcitation increases the chain radius.

Figure 5 further shows that the instantaneous frequency of the A_1 phonon increases almost linearly with time (at least for the first few oscillations), i.e. the frequency is chirped. The chirp means that the 'instantaneous frequency' of the phonon drifts in time. At higher fluence the initial instantaneous frequency softens and the chirp decay time increases. This suggests that the chirp is caused by a continuous reduction of the surface carrier density by the diffusion normal to the crystal surface and not by damping of the phonon amplitude, which would lead to a decrease of the anharmonicity thus increasing the frequency with successive cycles of the oscillations. As can be easily shown [15] the expected time dependence of the plasma density is likely to be the most important effect and the observed variations in the frequency of coherent A_1 oscillations can be very well understood in terms of this alone, without any explicit dependence of the phonon frequency on the coherent amplitude. Therefore, while true anharmonicity (that is, an explicit dependence of the phonon frequency on the phonon amplitude as is the case for Bi [3, 17]) may contribute to some extent, the present experiments can be explained in terms of the expected effects of a time-dependent plasma density.

Finally we note that in a striking contrast to the data presented in figure 1, the oscillatory signal in figure 5 is almost two orders of magnitude larger. This is because in the isotropic

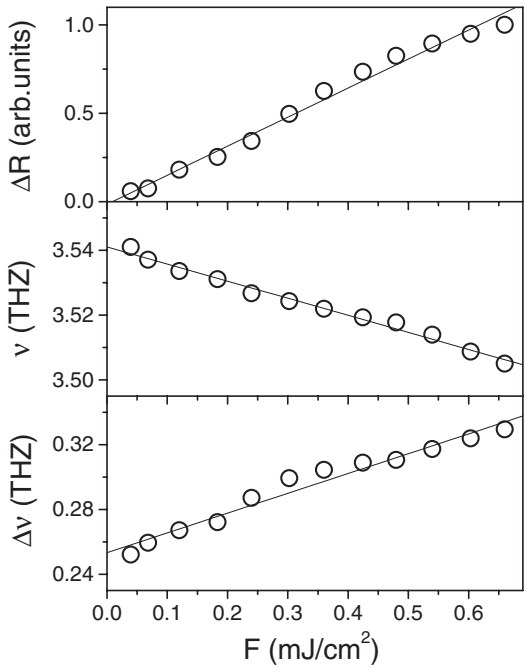

Figure 5. Pump dependence of the A_1 oscillation obtained from the *bc* face with conventional (isotropic) sampling.

detection scheme the signal is proportional to the squared matrix element instead of the squared difference of matrix elements in the anisotropic detection scheme.

In conclusion, we have measured the response of Te to ultrafast photoexcitation achieved for different crystallographic directions with the use of sub-picosecond laser pulses. We observed both fully symmetric and doubly degenerate coherent phonons that obey the selection rules prescribed by a second-rank Raman tensor. In addition, in the time domain the doubly degenerate phonons exhibit a splitting between LO and TO modes that is difficult to observe in the frequency domain. In the time domain the interaction with an intense pump pulse induces high density electron plasma which hybridizes with LO phonons. For the coupled phonon–plasmon mode, the contributions from the deformation potential mechanism and from the electro-optic mechanism have either the same sign or a different magnitude, thus preventing their cancellation. In the frequency domain, the carrier density is too low, the hybridization is weak, and, as a result, the contribution from the deformation potential mechanism exactly cancels that from the electro-optic mechanism due to their different signs. Finally, varying the pump fluence we observed that the frequency of the A_1 phonon redshifts to lower energy and is chirped even in a low fluence regime. The observed variations in the frequency and chirp of coherent A_1 oscillations can be very well understood in terms of the time dependence of the plasma density alone, without any explicit dependence of the phonon frequency on the coherent amplitude.

Acknowledgments

We thank M Wuttig and P Grosse for providing single-crystal Te samples. This work was supported in part by NATO (grant PST.GLG.978935), as well as by the Deutsche

Forschungsgemeinschaft (grant DE 567/9) and the Russian Foundation for Basic Research (grant 04-02-97204).

References

[1] Cavalleri A, Toth S, Siders C M, Squier J A, Raksi F, Forget P and Kiefer J C 2001 *Phys. Rev. Lett.* **87** 237401
[2] Misochko O V 2001 *Zh. Exp. Teor. Fiz.* **119** 285
Misochko O V 2001 *JETP* **92** 246 (Engl. Transl.)
[3] Misochko O V, Hase M, Ishioka K and Kitajima M 2004 *Phys. Lett.* A **321** 382
[4] Merlin R 1997 *Solid State Commun.* **102** 207
[5] Dekorsy T, Cho G C and Kurz H 2000 *Light Scattering in Solids* vol 8, ed M Cardona and G Güntherodt (Berlin: Springer) p 169
[6] Pine A S and Dresselhaus G 1971 *Phys. Rev.* B **4** 356
[7] Richter W 1972 *J. Phys. Chem. Solids* **33** 2123
[8] Cheng T K, Vidal J, Zeiger M J, Dresselhaus G, Dresselhaus M S and Ippen E P 1991 *Appl. Phys. Lett.* **59** 1923
[9] Dekorsy T, Auer H, Bakker H J, Waschke C, Roskos H G, Kurz H, Wagner W and Grosse P 1995 *Phys. Rev. Lett.* **74** 738
[10] Hunsche S, Wienecke K, Dekorsy T and Kurz H 1995 *Phys. Rev. Lett.* **75** 1815
[11] Dekorsy T, Auer H, Bakker H J, Roskos H G and Kurz H 1996 *Phys. Rev.* B **53** 4005
[12] Kim A M-T, Roeser C A D and Mazur E 2003 *Phys. Rev.* B **68** 012301
[13] Cardona M and Güntherodt G (ed) 1982 *Light Scattering in Solids II. Basic Concepts and Instrumentation* (Berlin: Springer)
[14] Lucovsky G, Keezer R C and Burstein E 1967 *Solid State Commun.* **5** 439
[15] Tangney P and Fahy S 2002 *Phys. Rev.* B **65** 054302
[16] Hsueh H C, Lee C C and Wang C W 2000 *Phys. Rev.* B **61** 3851
[17] Hase M, Kitajima M, Nakashima S and Mizoguchi K 2002 *Phys. Rev. Lett.* **88** 067401
[18] Grosse P and Richter W 1983 *Physics of Non-Tetrahedrally Bonded Elements and Binary Compounds I* (*Landolt–Börnstein New Series* Group III, vol 17) ed O Madelung (Berlin: Springer)